Quantifying Confounding Effect of Co-pathologies in Neurodegenerative Diseases with sensGAN

Yifan Lin
Department of Biostatistics
University of Washington
yifanlin@uw.edu

Kevin Z. Lin
Department of Biostatistics
University of Washington
kzlin@uw.edu

Single-cell RNA sequencing (scRNA-seq) offers detailed insight into the cellular mechanisms of neurodegeneration, including Alzheimer's disease (AD). Identifying AD-specific gene expression changes requires adjusting for covariates like age and sex. However, a major challenge lies in unmeasured co-pathologies – other neurodegenerative diseases (ND) that commonly co-occur with AD (10). For instance, in late-onset AD, only 31% of cases are described with AD-specific signatures (12), while most AD donors bear multiple NDs. The difficulty in measuring biomarkers for different NDs and the evolving definitions of NDs (7) pose substantial challenges to collecting co-pathology information. These co-pathologies can distort transcriptomic profiles and, when unaccounted for, introduce bias and confounding in biomarker discovery efforts (13). We aim to adjust differential expression (DE) p-values for unmeasured co-pathologies to identify candidate genes responding directly to AD-specific pathologies. Our analysis helps the researchers to hone in on therapeutic targets that directly mitigate the impact of AD pathological burden on cellular function.

Sensitivity analysis quantifies the potential impact of the omitted variable bias (OVB) on coefficient estimates. A sensitivity analysis addresses how "extreme" an unmeasured confounder would need to be to nullify the significance of a treatment-outcome relation. Our work is interested in understanding how AD pathology ("treatment") impacts a cell's function, measured through gene expression ("outcome"). In one relevant field of work driven by the worst-case bias, OVB for linear models is reparameterized with partial R^2 for the case-control and outcome variable to estimate the worst-case bias (1). This reparameterization explicitly describes an inverse relationship between a treatment's decreased significance on the outcome (adjusted for an unmeasured confounder) and the increased predictive power the unmeasured confounder has on the treatment or outcome. However, such methods are not easily generalizable to the setting of high-dimensional outcomes, such as analyzing the entire transcriptome at once. In another field of work, Surrogate Variable Analysis (SVA) assumes that residual variation can be effectively captured by low-dimensional surrogate variables (8; 9). In genomic studies, methods such as CATE (14) and GCATE (4) have been developed to enable large-scale hypothesis testing in the presence of confounding, while causarray (3) achieves robust statistical estimation of treatment effects accounting for latent confounding. However, these methods do not account for potential confounder-treatment relations or the worst-case confounding.

Our method, **sensGAN** (Sensitivity Generative Adversarial Network), quantifies the impact of unmeasured confounder $\boldsymbol{Z} \in \mathbb{R}^{n\times k}$ (i.e., co-pathology burden) among n donors based on average prediction gains of the case-control status $\boldsymbol{D} \in \{0,1\}^n$ (i.e., AD pathology as treatment) and the pseudobulk transcriptomic profile $\boldsymbol{Y} \in \mathbb{R}^{n\times p}$ (i.e., outcomes). Predictive gains are quantified by McFadden's R^2. Additional covariate of interests such as sex and APOE genetics are denoted by $\boldsymbol{X} \in \mathbb{R}^{n\times d}$ (Fig. 1A). Motivated by the theory of sensitivity analyses that define the change in significance constrained by the predictive power of $\boldsymbol{Z}$, we use two baseline components to quantify the original predictive power (Fig. 1B). Component ① is a fully connected (FC) 1-layer neural network (NN) with softmax loss. Component ② is a FC one-layer NN with a negative binomial (NB) log-likelihood loss. The baseline predictive powers are later used to calculate the predictive gains, which remain below fixed thresholds. As we will show, this baseline aids in interpreting how "direct" a gene responds to AD pathology, as opposed to the unmeasured co-pathology.

We adopted a GAN framework to learn an unmeasured confounder that could potentially eliminate the significance of AD pathology on a particular gene's expression. Specifically, sensGAN identifies the confounder that nullifies the most number of significant DE genes, while limiting the predictive gains that accounted for confounding (Figure 1C). Then, we train the deep-learning framework in an adversarial fashion, which comprises two groups of NNs - the predictor networks and the generator network. The predictor networks (components ③, ④) use a learned unmeasured confounder $\boldsymbol{Z}$ along with other variables to predict both $\boldsymbol{D}$ and $\boldsymbol{Y}$. Components ③ and ④ structurally mirror components ① and ②. The generator network (component ⑤) that learns the worst-case $\boldsymbol{Z}$ and component ⑤ is a 2-layer NN with ReLU activation function. Given a learned $\boldsymbol{Z}$, the predictor networks mirror the baseline networks, quantifying the

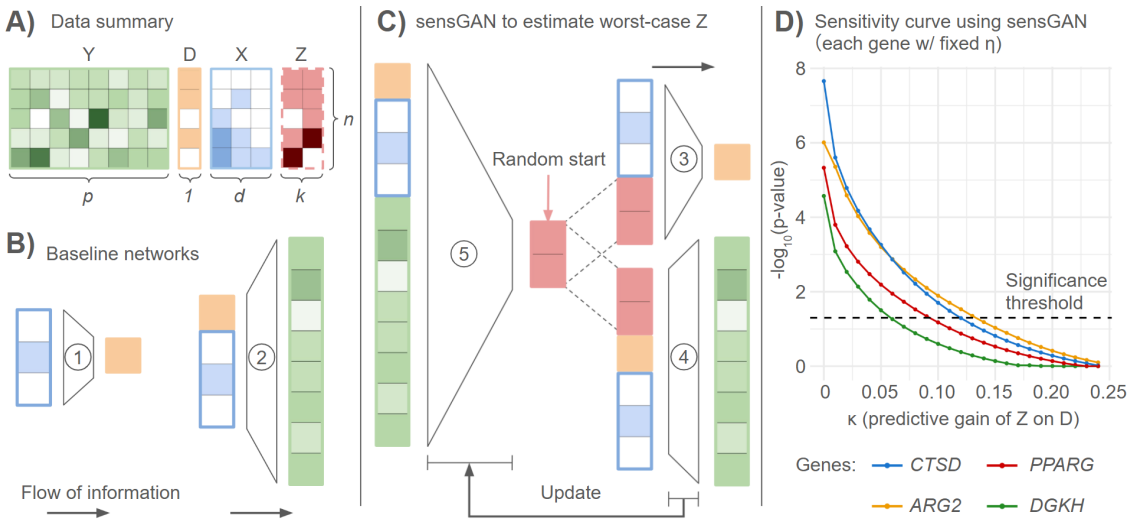

Figure 1: **A)** Schematic of data, involving a gene expression matrix $\boldsymbol{Y}$ (i.e., outcomes), a case-control variable $\boldsymbol{D}$ (i.e., treatment), other measured covariates $\boldsymbol{X}$, and unmeasured confounders $\boldsymbol{Z}$. **B)** The baseline networks ① and ② quantifying predictive power of the $\boldsymbol{D}$ and $\boldsymbol{Y}$. **C)** GAN to learn a $\boldsymbol{Z}$ with limited predictive gains, yielding a minimum number of DE genes. Components ③ and ④ quantify the predictive power of a given $\boldsymbol{Z}$ while ⑤ learns an appropriate $\boldsymbol{Z}$. While ⑤ is randomly initialized (yielding a random $\boldsymbol{Z}$), the iterative training between ③, ④, and ⑤ eventually yields the worst-case $\boldsymbol{Z}$. **D)** Sensitivity curve showing the worst-case p-value with varying predictive gains of the case-control variable for 4 genes, holding η fixed for each gene as κ changes.

predictive power but accounting for the confounder. Predictive gains are calculated as $R^2_{\text{McF},D}$ and $R^2_{\text{McF},Y}$. Then, the generator network finds a $\boldsymbol{Z}$ such that: (1) the predictive gain of $\boldsymbol{X}$, $\boldsymbol{Z}$ on $\boldsymbol{D}$ quantified by $R^2_{\text{McF},D}$ is below a fixed threshold κ, (2) that of $\boldsymbol{X}$, $\boldsymbol{D}$, $\boldsymbol{Z}$ on $\boldsymbol{Y}$ quantified by $R^2_{\text{McF},Y}$ is below a fixed threshold η, and (3) a full model with $\boldsymbol{Z}$ yields the minimum number of significant genes for the significance level α. The predictive gains exceeding predefined thresholds are penalized, and a sigmoid transformation is applied within the objective function to ensure differentiability for backpropagation. Therefore, our objective function is:

$$\min \left\{ \frac{1}{p} \left[\sum_{j=1}^{p} \sigma_{\lambda_{\text{GLM}}} \left(\left| \frac{\widehat{\beta}_j}{\text{SE}(\widehat{\beta}_{j,\text{res}})} \right| - \Phi^{-1}(1-\alpha) \right) \right] + \sigma_{\lambda_D} \left(R^2_{\text{McF},D} - \kappa \right) + \sigma_{\lambda_Y} \left(R^2_{\text{McF},Y} - \eta \right) \right\},$$

where $\widehat{\beta}_{j,\text{res}}$ denotes the case-control effect coefficient for gene j estimated *without* adjusting for confounding, and $\widehat{\beta}_j$ is the corresponding estimate *with* confounding adjustment. Here, $\lambda_{\text{GLM}}, \lambda_D, \lambda_Y \geq 0$ are hyperparameters for the temperature of their respective sigmoid functions, and $\Phi^{-1}(1-\alpha)$ represents the critical value of the standard normal distribution for a two-sided test at significance level α. To compute the DE p-value of gene j adjusting for $\boldsymbol{Z}$, we assume that $\text{SE}(\widehat{\beta}_{j,\text{res}}) \approx \text{SE}(\widehat{\beta}_j)$, so we can model the DE test statistic $|\widehat{\beta}_j / \text{SE}(\widehat{\beta}_{j,\text{res}})|$ as a z-score.

As proof of concept, we tested our method on the SEA-AD dataset (6), specifically on pseudobulk scRNA-seq data of microglia in the mid-temporal gyrus brain region from 78 donors, where $\boldsymbol{D}$ denotes the presence of clinically significant AD pathology defined by amyloid-β plaques and neurofibrillary tangles (21 controls, 57 cases). We believe the impact of co-pathologies would not exceed that of sex and APOEε4 status in AD. Therefore, we fix η for each gene based on a GLM-NB model with these known covariates. Figure 1D showcases that the significance of different genes is nullified at varying levels of κ, where genes being nullified at a larger value of κ are potentially responding to specifically AD pathology as opposed to a confounding co-pathology. For instance, a larger κ (0.13) is needed to explain away the effect of AD pathology on the expression of *ARG2* (arginase-2), suggesting fluctuations in arginase is more directly responding to AD pathology (11). In contrast, *DGKH* (diacylglycerol kinase η) is significant, assuming there are no unmeasured confounders, but becomes insignificant with a smaller value of κ (0.06). This is potentially because *DGKH* has been implicated with bipolar disorder (15), which has been shown to overlap with AD (2).

Moving forward, our goals include further validating sensGAN on a different biological system (16). We plan to withhold observed donor covariates, perform confounder estimation, and compare the estimated confounders and withheld covariates. We also seek to extend categorical confounder adjustments from the pseudo-bulk to the single-cell resolution and extend sensGAN not to require pseudobulking scRNA-seq data. Altogether, sensGAN will help identify novel changes in cell-type functions responding to any particular ND while adjusting for unmeasured co-pathologies.

References

[1] CINELLI, C., AND HAZLETT, C. Making sense of sensitivity: Extending omitted variable bias. *Journal of the Royal Statistical Society Series B: Statistical Methodology 82*, 1 (2020), 39–67.

[2] DRANGE, O. K., SMELAND, O. B., SHADRIN, A. A., FINSETH, P. I., WITOELAR, A., FREI, O., GROUP, P. G. C. B. D. W., WANG, Y., HASSANI, S., DJUROVIC, S., ET AL. Genetic overlap between Alzheimer's disease and bipolar disorder implicates the MARK2 and VAC14 genes. *Frontiers in Neuroscience 13* (2019), 220.

[3] DU, J.-H., SHEN, M., MATHYS, H., AND ROEDER, K. Causal differential expression analysis under unmeasured confounders with causarray. *bioRxiv* (2025), 2025–01.

[4] DU, J.-H., WASSERMAN, L., AND ROEDER, K. Simultaneous inference for generalized linear models with unmeasured confounders. *Journal of the American Statistical Association*, just-accepted (2025), 1–24.

[5] FILIPPOVA, G. N., CASAD, M., GRONECK, C., HUI, K., MISHRA, S., MACDONALD, J. W., BAMMLER, T., VAN DYKE, D. L., SKAKKEBAEK, A., GRAVHOLT, C. H., ET AL. Modeling sex differences in Alzheimer's disease using isogenic hiPSC lines with different sex chromosome complements and APOE alleles. *Alzheimer's & Dementia 20*, Suppl 1 (2025), e093548.

[6] GABITTO, M. I., TRAVAGLINI, K. J., RACHLEFF, V. M., KAPLAN, E. S., LONG, B., ARIZA, J., DING, Y., MAHONEY, J. T., DEE, N., GOLDY, J., ET AL. Integrated multimodal cell atlas of Alzheimer's disease. *Nature Neuroscience 27*, 12 (2024), 2366–2383.

[7] JACK JR, C. R., ANDREWS, J. S., BEACH, T. G., BURACCHIO, T., DUNN, B., GRAF, A., HANSSON, O., HO, C., JAGUST, W., MCDADE, E., ET AL. Revised criteria for diagnosis and staging of Alzheimer's disease: Alzheimer's Association Workgroup. *Alzheimer's & Dementia 20*, 8 (2024), 5143–5169.

[8] LEEK, J. T., AND STOREY, J. D. Capturing heterogeneity in gene expression studies by surrogate variable analysis. *PLoS genetics 3*, 9 (2007), e161.

[9] LEEK, J. T., AND STOREY, J. D. A general framework for multiple testing dependence. *Proceedings of the National Academy of Sciences 105*, 48 (2008), 18718–18723.

[10] NICHOLS, E., MERRICK, R., HAY, S. I., HIMALI, D., HIMALI, J. J., HUNTER, S., KEAGE, H. A. D., LATIMER, C. S., SCOTT, M. R., STEINMETZ, J. D., WALKER, J. M., WHARTON, S. B., WIEDNER, C. D., CRANE, P. K., KEENE, C. D., LAUNER, L. J., MATTHEWS, F. E., SCHNEIDER, J., SESHADRI, S., WHITE, L., BRAYNE, C., AND VOS, T. The prevalence, correlation, and co-occurrence of neuropathology in old age: Harmonisation of 12 measures across six community-based autopsy studies of dementia. *The Lancet Healthy Longevity 4*, 3 (2023), e115–e125.

[11] OVSEPIAN, S. V., AND O'LEARY, V. B. Can arginase inhibitors be the answer to therapeutic challenges in Alzheimer's disease? *Neurotherapeutics 15*, 4 (2018), 1032–1035.

[12] ROBINSON, J. L., XIE, S. X., BAER, D. R., SUH, E., VAN DEERLIN, V. M., LOH, N. J., IRWIN, D. J., MCMILLAN, C. T., WOLK, D. A., CHEN-PLOTKIN, A., ET AL. Pathological combinations in neurodegenerative disease are heterogeneous and disease-associated. *Brain 146*, 6 (2023), 2557–2569.

[13] SANTIAGO, J. A., AND POTASHKIN, J. A. The impact of disease comorbidities in Alzheimer's disease. *Frontiers in Aging Neuroscience 13* (2021), 631770.

[14] WANG, J., ZHAO, Q., HASTIE, T., AND OWEN, A. B. Confounder adjustment in multiple hypothesis testing. *Annals of statistics 45*, 5 (2017), 1863.

[15] WHALLEY, H. C., PAPMEYER, M., ROMANIUK, L., JOHNSTONE, E. C., HALL, J., LAWRIE, S. M., SUSSMANN, J. E., AND MCINTOSH, A. M. Effect of variation in diacylglycerol kinase eta (DGKH) gene on brain function in a cohort at familial risk of bipolar disorder. *Neuropsychopharmacology 37*, 4 (2012), 919–928.

[16] YAZAR, S., ALQUICIRA-HERNANDEZ, J., WING, K., SENABOUTH, A., GORDON, M. G., ANDERSEN, S., LU, Q., ROWSON, A., TAYLOR, T. R., CLARKE, L., ET AL. Single-cell eQTL mapping identifies cell type-specific genetic control of autoimmune disease. *Science 376*, 6589 (2022), eabf3041.